Article

Journal of the Brazilian Chemical Society

https://dx.doi.org/10.21577/0103-5053.20230154

J. Braz. Chem. Soc. **2024**, *35*, 4, e-20230154, 1-15

A Multi-Geochemical Characterization to Evaluate Anthropogenic Contamination in Marine Sediments from Port of Suape, Northeast of Brazil

Ana Flávia B. de Oliveira,[a] Bruna R. S. Gomes,[a] Rebeca S. França,[b] Thayane Cristina S. Moreira,[a] Alex S. Moraes,[a] Giovana A. Bataglion[b] and Jandyson M. Santos[*,a]*

[a]*Grupo de Pesquisa em Petróleo, Energia e Espectrometria de Massas (PEM), Departamento de Química, Universidade Federal Rural de Pernambuco (UFRPE), 52171-900 Recife-PE, Brazil*

[b]*Departamento de Química, Instituto de Ciências Exatas, Universidade Federal do Amazonas (UFAM), 69077-000 Manaus-AM, Brazil*

To investigate the anthropogenic contamination of the Port of Suape, five surface sediments were collected and subjected to a geochemical characterization based on the determination of environmental biomarkers such as sterols, aliphatic and polycyclic aromatic hydrocarbons, and also metals and arsenic. Sterol analyses point to a moderate level of sewage contamination, while *n*-alkanes analyses indicated contamination by petroleum in an early stage of biodegradation. Polycyclic aromatic hydrocarbons analyses pointed to a mixture of contributions for the organic matter, which were predominantly found for petrogenic and pyrolytic sources. The quantification of trace metals indicated a low risk to the environment, except for As, which was identified as displaying moderate contamination. During the analysis of all biomarkers, the sediment collected near one of the shipyards was the most affected. These results enable comprehension of the level of contamination in an important Brazilian port and the need to develop remediation policies.

Keywords: environmental biomarkers, sterols, hydrocarbons, sediments, port of Suape

Introduction

Estuaries are aquatic environments that arise from the transition between rivers and seas and are strongly influenced by anthropogenic activities such as fishing, tourism, and industrial and port activities.[1] Port activities may introduce contaminants into the environment, such as domestic and industrial sewage, petroleum products, metals, and persistent organic pollutants.[2] These pollutants are often associated with activities such as ship repair and maintenance, dredging of the access channels, atmospheric emissions, and the generation of solid and liquid effluents from ships entering and leaving the port.[3] The geochemical characterization of sediments has been a prominent tool over the years, as it provides data about the contamination of a given environment, allowing for the determination of its composition and source.[4]

One of the main sources of environmental contamination found in sediments is sewage, which can be assessed through sterol analysis.[5] Sterols are hydrophobic (lipidic) compounds that serve as biomarkers of sewage contamination due to their high specificity to fecal materials, with a predominance in human feces, and their resistance to degradation.[6] Inappropriate disposal of sewage in the environment can generate an increase in organic matter (OM), eutrophication, ecosystem instability due to the reduction of species and the proliferation of toxic algae.[7] These impacts not only pose risks to the environment but also have implications for human health. Hence, monitoring these biomarkers becomes crucial for effective environmental assessment.

Along with sewage, the release of oil and its derivatives poses a significant source of aquatic contamination and can be investigated through sediment analysis.[8] This contamination can arise from river discharges, navigation activities, oil transfer through pipelines, and the combustion of fossil fuels.[4,9] Due to the toxic characteristics of this contamination, high concentrations in aquatic environments can cause damage to biota and human beings. The use of markers such as aliphatic hydrocarbons (AHs) and polycyclic aromatic hydrocarbons (PAHs) has been successful in tracking environmental pollution.[4,8,10,11]

*e-mail: jandyson.machado@ufrpe.br
Editor handled this article: Maria Cristina Canela (Associate)

Furthermore, while trace metals are naturally found in aquatic systems, the main sources of these substances in the environment are industrial activities and sewage disposal.[12,13] Trace metals have a tendency to remain well-preserved in sediments over time, representing a significant threat to human health due to their highly toxic nature, even in low concentrations.[14] Regions located near industrial zones have a high risk of exposure to toxic metals, which can result in health damage such as kidney disease, cancer, and miscarriage, in addition to causing significant ecological damage.[15] In estuarine regions, geochemical analyses of metals such as copper (Cu), lead (Pb), nickel (Ni), and zinc (Zn) in sediments can provide information about their distribution and sources, indicating the environmental health of a region.[16]

The Port of Suape, located in the Northeast region of Brazil, is recognized as one of the most significant ports in the country. Since its establishment between 1979 and 1984, it has played a crucial role in facilitating industrial and navigation activities.[17] This port complex is situated near the estuaries of the Tatuoca and Massangana rivers, and it serves as a daily transit point for various cargo ships, as well as operating shipyards. Although some studies[18,19] have been carried out investigating the presence of anthropogenic contamination in the Port of Suape, based on our current understanding, no study has been conducted to assess multiple biomarkers, especially sterol compounds.

The objective of this study was to comprehensively characterize the sediments in the Suape Industrial Port Complex using a multi-geochemical approach. The goal was to evaluate sediment quality and determine the extent of contamination in an area heavily influenced by navigation traffic and shipyard activities. To achieve these objectives, a range of analyses were employed, including infrared spectroscopy, analysis of OM, elementary composition, and grain size. Furthermore, analytical techniques were conducted to determine various classes of biomarkers such as sterols, AHs, and PAHs, as well as trace metals and arsenic (As).

Experimental

Sampling collection and pretreatment procedures

A total of five surface sediment samples (0-10 cm) were collected from the Suape Industrial Port Complex (Figure 1 and Table S1, Supplementary Information (SI) section) located in the municipality of Ipojuca, in September 2018. Access to the port region is controlled by government authorities, which hindered an extensive collection of a larger quantity of samples. Samples P1 and P2 were collected near two different shipyards in operation since 2009 and 2013, respectively. The region of sample P3 is located on the Massangana River where mangrove vegetation predominates. In this region, there are also hotel activities and bars in the area, as well as small boats using a pier and bathing activities. Sample P4 was located near Suape Beach, in an area protected by a natural reef barrier, which makes the sea calm and suitable for fishing activities. Sample P5 was collected in a region with heavy navigation

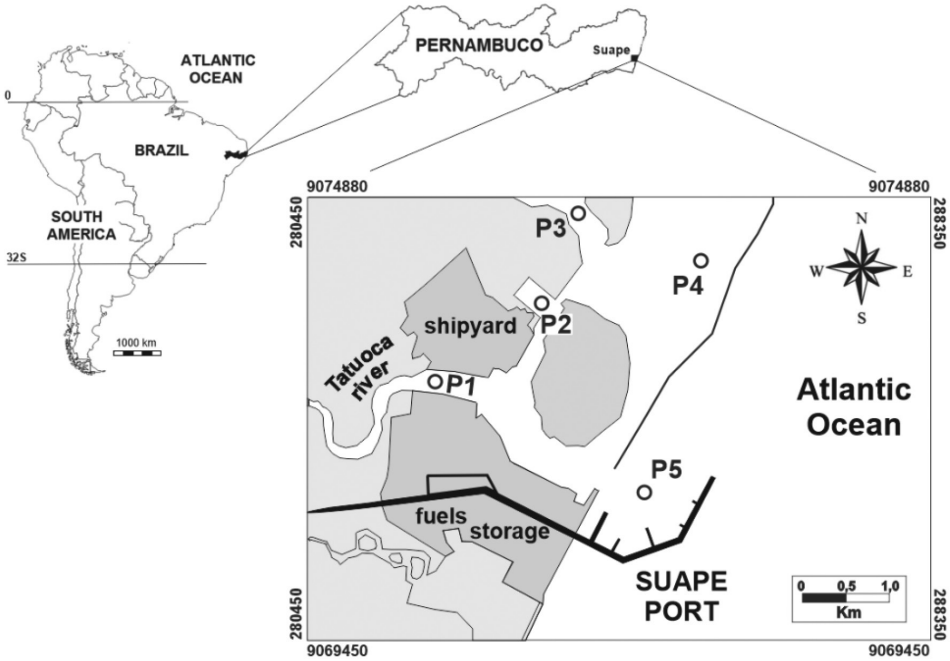

Figure 1. Study area and sampling points in the Suape Industrial Port Complex, Pernambuco, Brazil.

traffic, located near the waterway terminal, which has four docks that mainly carry out the loading/unloading of products such as diesel oil, crude oil, liquified petroleum gases, fuel oil, and aviation kerosene.

From each sampling site within the study area, approximately 300 g of sediment were collected using a Van Veen sampler and were carefully transferred to pre-cleaned glass bottles. The collected samples were immediately transported under low-temperature conditions (4 ºC) to the laboratory. The samples were dried in lyophilizer for 24 h and were subsequently finely ground using a porcelain mortar and pestle, followed by sieving to obtain particles smaller than 2 mm. Finally, the sieved sediments were stored at room temperature for further analysis.[7]

Chemicals and reagents

High-performance liquid chromatography (HPLC)-grade solvents (dichloromethane, *n*-hexane, and methanol) were obtained from Tedia (Rio de Janeiro, Brazil). Hydrochloric acid and metallic copper were purchased from Vetec (Rio de Janeiro, Brazil) and Dinâmica Química Contemporânea (Indaiatuba, SP, Brazil), respectively. Coprostanol (3β,5β-cholestan-3-ol), cholesterol (3β-cholest-5-en-3-ol), epicoprostanol (3α,5β-cholestan-3-ol), cholestanol (3β,5α-cholestan-3-ol), stigmasterol (3β,22*E*)-ethycholest-5,22-dien-3-ol), campesterol (3β,24*R*-methycholest-5-en-3-ol), β-sitosterol (24-ethycholest-5-en-3β-ol), stigmastanol (3β,5α-ethycholest-3-ol), brassicasterol ((3β,22*E*)-methycholest-5,22-dien-3-ol), ergosterol ((3β,22*E*)-ergosta-5,7,22-trien-3-ol) and cholesterol-d_6 were purchased from Sigma-Aldrich (St. Louis, USA). Dichloromethane was used to prepare stock solutions of individual sterols at a concentration of 1.0 mg mL^{-1}. Subsequently, working standard solutions containing all sterols at 2.0 μg mL^{-1} were prepared by diluting the stock solutions in methanol. Deuterated standards *n*-triacontane-d_{62}, *p*-terphenyl-d_{14}, *n*- hexadecane-d_{34}, and alkanes (*n*-C_7-*n*-C_{40}) were obtained from Sigma-Aldrich (St. Louis, MO, USA). The PAHs standard and PAHs deuterated standard mixtures were acquired from AccuStandard (New Haven, CT, USA) (Table S2, SI section). Inductively coupled plasma (ICP) standard multi-element solution IV CertiPUR was obtained from Merck (Darmstadt, HE, Germany).

Characterization of sediments and bulk analyses

The sediment samples were subjected to analysis using mid-infrared spectroscopy (400-4000 cm^{-1}) with an IR TRACER-100 Fourier Transform spectrometer (Shimadzu Co., Kyoto, Japan) at a resolution of 4 cm^{-1} (Shimadzu Co., Kyoto, Japan). As previously described in Oliveira *et al.*,[6] a grail and agate pistil were used to macerate 1 mg of sediment with KBr, which were subjected to compression using a hydraulic press. All infrared data were normalized in the processing.

The organic matter content was evaluated by gravimetry after calcination at approximately 750 ºC for 4 h, as outlined in a previous study.[20]

The elementary analysis was carried out following the methodology described by Oliveira *et al.*[6] Briefly, decarbonization of each sediment sample (1 g) was conducted by sequential treatment with a 0.1 mol L^{-1} hydrochloric acid solution, followed by rinsing with deionized water. Subsequently, the sediments were dried at 60 ºC and subject to analysis using a CHN628 (LECO Co., USA) equipped with Software CHN628 version 1.30. The instrument was previously calibrated using an ethylenediaminetetraacetic acid (EDTA) standard (41.0% C, 5.5% H, and 9.5% N).

The grain size analysis was performed following the method proposed by Suguio[21] and consisted of two steps: (*i*) the separation between the fine particles (silt + clay) and the sand particles was carried out through sieving (0.063 mm); (*ii*) the separation of the sediment into silt and clay fractions was carried out using the pipetting technique based on the Stokes principle.

Extraction and fractionation of sediments

The extraction and fractionation procedure of the organic compounds was performed as described by Rau *et al.*[22] In summary, activated copper and internal standard (IS) were added to 10 g of sediment. As IS, we have used the cholesterol-d_6 for sterols (2 μg g^{-1}), *n*-triacontane-d_{62} for *n*-alkanes (0.2 μg g^{-1}), and *p*-terphenyl-d_{14} for PAHs (10 ng g^{-1}). The sediment samples were extracted using 20 mL of a mixture of dichloromethane and methanol (2:1, v/v) involving vortexing and ultrasonic treatment, and the procedure was repeated two times more. After combining the three organic extracts, rotary evaporation was employed to remove the solvents, followed by drying with N_2 flow. The extract was then fractionated using open column chromatography prepared by packing 10 g of silica gel and 1 g of alumina, both previously dried at 150 and 450 ºC, respectively, and disabled with 5% deionized water. Three fractions (named F1, F2, and F3) of the organic extract were obtained, as follows: fractions of AHs eluted with 40 mL of *n*-hexane (F1), PAHs eluted with 30 mL of *n*-hexane:dichloromethane (1:1, v/v) (F2), alcohols and sterols eluted with 30 mL of ethyl acetate:methanol (2:1, v/v) (F3). The F1,

F2, and F3 fractions underwent analysis using gas chromatography with flame ionization detection (GC-FID), gas chromatography-mass spectrometry (GC-MS), and liquid chromatography-tandem with mass spectrometry (LC-MS/MS), respectively.

Determination of AH and PAHs

The determination of AHs (F1) was conducted using GC-FID model 2010 (Shimadzu, Kyoto, Japan) equipped with autosampler model AOC-20s, an auto-injector model AOC-20i (Shimadzu, Kyoto, Japan) and a capillary column HT-5 (25 m, 0.32 mm internal diameter, 0.10 µm film thickness) (Trajan Scientific and Medical, Ringwood, VIC, Australia). The injection volume (1.0 µL) was in the splitless mode under the specified conditions: nitrogen as carrier gas at 1.70 mL min^{-1} and temperature program at 60 ºC for 5 min, increasing by 5 ºC min^{-1} to 330 ºC (held for 5.0 min).

The determination of PAHs (F2) was carried out using GC-MS model QP2010 (Shimadzu, Kyoto, Japan) equipped with autosampler model AOC-20s, an auto-injector model AOC-20i (Shimadzu, Kyoto, Japan) and capillary column RTX-5MS (30 m, 0.25 µm film thickness 0.25 mm internal diameter) (Restek, Bellefonte, PA, USA), with electron ionization (70 eV) and single quadrupole analyzer. The injection volume of 1.0 µL was performed in splitless mode with the following conditions: helium was used as the carrier gas at a flow rate of 1.0 mL min^{-1}, a temperature program starting at 60 ºC for 5 min, increasing by 5 ºC min^{-1} to 300 ºC (held for 10.0 min). The ion source temperatures, injector, and transfer line were at 200, 280, and 300 ºC, respectively. PAHs were detected using the analysis mode of selected ion monitoring (SIM), focusing on the molecular ions as listed and summarized in Table S2.

Determination of sterols

The analysis of sterols (F3) was conducted using LC-MS/MS with a liquid chromatography 1200 Series system (Agilent, Santa Clara, USA) coupled to an API 4000 QTrap mass spectrometer (Applied Biosystems, Darmstadt, Germany). The mass spectrometer was equipped with atmospheric pressure chemical ionization (APCI) and operated in the positive ion mode acquisition.

Ten sterols were investigated (coprostanol, epicoprostanol, cholesterol, cholestanol, campesterol, stigmasterol, β-sitosterol, stigmastanol, brassicasterol, and ergosterol) and the LC-MS/MS conditions were previously described in Oliveira *et al*.[6] Briefly, chromatographic separation was conducted in a Shimpack XR-ODS octadecyl-C18 reverse phase column (150 mm column length, 2.0 mm inner diameter and, 2.2 µm particle size. The mobile phases used for the analysis were methanol (mobile phase A) and water (mobile phase B). The gradient elution was carried out using the following program: 0-2 min (90% methanol), 2-8 min (100% methanol), 8-9 min (90% methanol), 9-10 min (90% methanol), at a flow rate of 0.6 mL min^{-1}. The injector temperature was set at 10 °C, while the chromatographic oven temperature was maintained at 30 °C. The injection volume was 10 µL. The APCI source was utilized with the following specific settings: corona current of 4.0 µA, temperature at 450 °C, and curtain gas at 10 (arb).

Determination of trace metals and As

Approximately 0.25 g of dried sediment was weighed and subjected to acid digestion with 18 mL of aqua regia (HNO_3:HCl, 1:3, v/v) into a digester block, heating at 85 °C for 2 h. At the end of the procedure, the samples were allowed to cool, and then filtered and measured to a volume of 25 mL in a volumetric flask. The samples were subjected to analysis using the inductively coupled plasma atomic emission spectrometry (ICP-OES) technique (Optima 7300DV model, PerkinElmer, USA) aiming at the detection of 11 elements: Cu, Pb, Ni, Zn, As, and silver (Ag), cadmium (Cd), chrome (Cr), cobalt (Co), tin (Sn), and vanadium (V).

Analytical parameters

The identification of sterols was performed using two precursor-product ion transitions for $[M + H - H_2O]^+$ ions and retention times obtained with authentic standards. The quantification of all compounds was achieved by calculating the response factors of the authentic standards relative to cholesterol-d_6. An analytical solution with a concentration of 2.0 µg mL^{-1} was prepared to generate the calibration curves, which were run in triplicate. The concentration range of each analyte varied from 20.0 to 1000.0 ng mL^{-1} (nine levels), and a concentration of 500.0 ng mL^{-1} for the internal standard.[23] The validation of the sterol method was carried out by obtaining the main analytical parameters, detailed previously by Bataglion *et al*.[24] The instrumental and chromatographic conditions can be found in Table S3 (SI section).

The identification of *n*-alkanes (AHs) was carried out by comparing the retention times of the samples with a standard solution containing the *n*-C_7 to *n*-C_{40} compounds. The quantification of *n*-alkanes was achieved by internal calibration using concentrations ranging from

1.0 to 50.0 μg mL^{-1}, with *n*-hexadecane-d_{34} as the internal standard. Each detected *n*-alkane was quantified using its corresponding analytical curve. Detailed analytical parameters for validating AHs can be found in Table S4 (SI section).

The identification of PAHs was carried out by comparing the molecular ions and retention times of the samples with a standard solution. The quantitative determination of PAHs was performed using internal calibration with concentrations ranging from 10.0 to 1000.0 ng mL^{-1}. Deuterated homologous internal standards were used at a concentration of 500.0 ng mL^{-1}, as listed in Table S2. Detailed analytical parameters for validating the PAHs can be found in Table S5 (SI section).

The quantitative determination of trace metals (Ag, As, Cd, Cr, Co, Cu, Ni, Pb, Sn, V, and Zn) and As was achieved through external calibration (1.0 to 1000.0 ng mL^{-1}), using the same acid matrix employed for the sediment analyses. Each element was quantified individually using its corresponding calibration curve. Quality control was performed using OREAS46 and OREAS47 (Ore Research & Exploration P/L, Chibougamau, Australia) as certified reference material. The analytical parameters obtained for the determination of trace metals and As are described in Table S6 (SI section).

Multivariate statistical analysis

The multi-geochemical results were processed by multivariate statistical analyses through Origin 8.0 software (free trial version),[25] as for the principal components analysis (PCA), and Heatmapper for hierarchical cluster analysis (HCA/Heatmap).[26] Statistical analyses were conducted using data obtained from bulk analyses (OM, total organic carbon (TOC), total organic carbon/total nitrogen (TOC/TN), sand, and silt + clay, in percentage) and for values of quantification of environmental biomarkers, trace metals and As.

For sterols, it was investigated the concentrations of coprostanol and its main diagnostic ratios coprostanol/cholesterol, and epicoprostanol/coprostanol), ((coprostanol/(coprostanol + cholestanol)). For AHs and PAHs, the main ratios were selected (terrestrial/aquatic ratio (TAR), carbon preference index (CPI), fluoranthene/fluoranthene + pyrene (Fl/Fl + Py), pristane/phytane, benz[*a*]anthracene/benz[*a*]anthracene + chrysene (BaA/228), anthracene/anthracene + phenanthrene (An/178), and Σlow molecular mass/Σhigh molecular mass (ΣLMM/ΣHMM). For trace metals and As, those with values above the quantification limit were selected (As, Cr, Cu, Ni, Pb, V, and Zn).

Results and Discussion

Bulk analyses

The infrared spectrum (Figure S1, SI section) showed bands associated with the typical chemical composition of sediments related to quartz, clay materials, and OM, as also was previously described by Oliveira *et al.*[6] In our study, it is worth highlighting two bands: a less intense one at 2973 cm^{-1} and a weak one at 2917 cm^{-1}. These can arise from the stretching vibrations, both asymmetric and symmetric of $-CH_3$ and $-CH_2$ related to aliphatic hydrocarbons, respectively.[27,28] Ng *et al.*[29] suggest that the intensity of these bands may be proportional to the level of contamination by hydrocarbons. In our study, they were prominent in sediments collected near the shipyards (P1 and P2 samples) and in the oil and gas loading/unloading area (P5 sample), which indicates possible contamination by hydrocarbons in these regions. A band at 2523 cm^{-1} was found in all samples, but more intense in P5, which is a band characteristic of S–H stretching, since few other absorptions occur in this region.[30]

The values of grain size, OM, and elementary analysis are summarized in Table 1. The grain size of the P1, P2, and P5 sediments consisted predominantly of fine particles (silt + clay) with percentages found from 54.1 to 69.5%. This result was as expected since in the regions of P1 and P2, maintenance dredging actions are applied to guarantee the depth of the access channel, enabling the movement of vessels of different sizes, while P5 sediment was collected in the open sea region, at a depth between 8 and 20 meters.[31]

Table 1. Results of OM, grain size and elementary analysis in percentage of surface sediments from Port of Suape

Sample	OM / %	Sand / %	Silt + clay / %	TOC / %	TN / %	TOC/TN	H / %	H/C
P1	22.33 ± 0.25	12.11	54.14	3.76	0.22	17.06	1.72	5.49
P2	25.73 ± 1.98	9.91	69.45	5.17	0.28	18.67	1.90	4.42
P3	9.49 ± 0.27	73.60	13.48	2.18	0.15	14.98	0.54	2.96
P4	6.57 ± 0.27	94.81	2.17	1.11	0.05	20.85	0.12	1.35
P5	22.17 ± 0.78	29.90	60.55	3.94	0.11	34.42	0.50	1.52

OM: organic matter; TOC: total organic carbon; TN: total nitrogen; H: hydrogen; C: carbon.

Environments with greater depths have lower hydrodynamic energy, and it is expected a higher percentage of fine particles.[22] P3 and P4 sediments are considered sandy with percentages equivalent to 73.60 and 94.81%, and it is due to the receipt of dredged material from nearby areas. Similar results with a predominance of sandy material due to the dredging process were also found in the particle size distribution of sediments from Vitória Bay Estuary, in the city of Vitória, state of Espírito Santo, Brazil.[32]

The percentages of OM range from 6.57 to 25.73%, which according to Gomes and Azevedo[33] can be inferred that all sediments analyzed in this study exhibit a high organic matter content, exceeding 0.5%. The OM showed a distribution pattern similar to that of fine particles, as seen in Mayer,[34] Muniz *et al*.[35] and Souza *et al*.[36] Based on this, a linear correlation between OM and fine particles was investigated and the result was obtained in a linear trend (R^2 = 0.9931). This indicates that the grain size of sediments, along with the low hydrodynamics of the area, influences the accumulation of OM[34,35] (Table S7, SI section).

The range of TOC values (1.11 to 5.17%) observed in the study area suggest varying OM inputs, potentially influenced by structural differences in local vegetation, resulting in a large addition of biomass to the soil or a large number of roots in the region.[37] As with OM, TOC showed a similar distribution to fine particles and because of this, a linear correlation was investigated (R^2 = 0.9539, Table S7). These results and the low hydrodynamics of the region[36] suggest that the particle size influences the accumulation of TOC in the region.[35] TN values (0.05 to 0.28%) in all sediments were below 1%, which suggests that the region was exposed to intense reducing conditions characterized by insufficient oxygen levels, which can facilitate the oxidation of nitrogenous compounds. Consequently, these compounds exist in their reduced form, which can be attributed to processes such as leaching caused by tidal cycles and subsequent denitrification.[38]

The TOC/TN can be used to differentiate among OM sources, where values between 4 and 10 indicate autochthonous sources and values greater than 20 indicate allochthonous sources.[8] The P1, P2, and P3 samples showed TOC/TN values between 14.98 and 18.67, which indicated that these regions have been subjected to a combination of contributions from vascular and non-vascular plants.[39] On the other hand, the TOC/TN ratios for P4 and P5 samples are 20.85 and 34.42, respectively, indicating that the OM came from vascular terrestrial plants (allochthones) with a high concentration of cellulose.[40,41] Note that relatively high TOC/TN values were found in all sediments, which may indicate sewage contamination due to carbon input from anthropogenic sources, in addition to suggesting that OM is difficult to degrade as stated by Grilo *et al*.[42] and Santos *et al*.[38] The H/C ratio of sediments characterizes them as having low aromaticity as their values were greater than 1. This result may be due to biogenic OM formed in water, arising from the decomposition of plankton, which is rich in lipids (non-aromatic compounds).[39]

Concentrations of sterol biomarkers

The results for the sterol concentrations can be found in Table 2. Eight sterols were detected with concentrations ranging from 1.51 to 40.72 μg g^{-1}, indicating a distinct sterol distribution in the samples. In addition, the diversity of sterols (fecal and biogenic) present in the sediments indicates that the OM came from different sources.[6]

The abundance of β-sitosterol in sediments P1, P2, and P3 suggests a large contribution of terrigenous OM (allochthonous), coming from vascular plants.[7,43] The contribution of phytosterols, such as stigmasterol and β-sitosterol, comes from the mangrove vegetation,[44] which is predominant in the Port of Suape region. Although the P3 region has the most predominant mangrove forests, the highest concentration of β-sitosterol was found in the P2 sediment (10.85 μg g^{-1}) located close to one of the shipyards,

Table 2. Absolute concentrations and diagnostic ratios of sterols in surface sediments from the Port of Suape, PE, Brazil

Sample	Cop / (μg g^{-1})	Epico / (μg g^{-1})	Colr / (μg g^{-1})	Coln / (μg g^{-1})	Camp / (μg g^{-1})	Stig / (μg g^{-1})	β-Sitr / (μg g^{-1})	Sitn / (μg g^{-1})	∑Sterols / (μg g^{-1})	R1 / %	R2	R3	R4	R5
P1	0.38	0.16	1.11	0.76	1.05	0.74	2.57	0.23	7.00	5.44	0.33	0.42	0.34	0.42
P2	7.76	1.50	2.71	4.70	5.11	4.78	10.85	3.31	40.72	19.05	0.62	0.66	2.86	0.19
P3	0.28	0.13	0.99	0.64	1.29	1.08	7.69	0.31	12.41	2.29	0.30	0.39	0.28	0.46
P4	0.10	0.17	0.59	0.24	0.44	0.18	0.50	< LOQ	2.22	4.67	0.29	0.53	0.17	1.70
P5	0.11	0.07	0.45	0.22	0.29	0.12	0.25	< LOQ	1.51	6.96	0.33	0.45	0.24	0.64

Cop: coprostanol; Epico: epicoprostanol; Cholr: cholesterol; Choln: cholestanol; Camp: campesterol; Stig: stigmasterol; β-Sitr: β-sitosterol; Sitn: sitostanol; R1: coprostanol/total sterols; R2: coprostanol/(coprostanol + cholestanol); R3: coprostanol + epicoprostanol/(coprostanol + epicoprostanol + cholestanol); R4: coprostanol/cholesterol; R5: epicoprostanol/coprostanol; LOQ: limit of quantification.

suggesting that this region receives an additional source of this sterol. According to Speranza *et al*.,[45] vegetable oils used in the kitchen have β-sitosterol in their composition, suggesting that sewage from the shipyard activities may compose the OM of this region.

In sediments P4 and P5, cholesterol was the most abundant sterol, indicating high aquatic productivity. This can be explained by a greater contribution of OM present in the open seawater area, as similarly reported by Bataglion *et al*.[43] Phytosterols were predominant in all sediments (44-84% of total sterols) corroborating the strong influence of terrigenous OM, thus supporting the idea that the areas receive a high contribution of biogenic OM.[46]

We applied several linear correlations between sterols of anthropogenic origin (coprostanol and epicoprostanol), biogenic origin (β-sitosterol and stigmasterol), and the results of bulk analyses, as shown in Table S7. No significant correlation was found between the aforementioned sterols and fine particles ($R^2 < 0.3$), suggesting that particle size is not a determining factor for the accumulation of sterols and that the region is influenced by different sources of OM.[47] An interesting linear correlation between these sterols and cholesterol ($R^2 > 0.75$) confirmed that organic material of fecal and terrigenous origin has influenced the formation of OM in the port region.[47] We also found a high correlation between coprostanol and epicoprostanol ($R^2 = 0.9963$), suggesting that these sterols had the same source, from sewage.[48]

In addition, we have found high values of OM (25.73%), TOC (5.17%), and TN (0.28%) in the P2 sediment. As this was the only sample that presented coprostanol concentrations surpassing the concentration of 0.50 μg g^{-1}, our finding suggested a direct or indirect considerable input of domestic sewage in the region. On the other hand, the P1, P3, P4, and P5 sediments presented concentrations between the range of 0.1-0.4 μg g^{-1}, indicating a moderate level of sewage contamination.[7,49] According to Bujagić *et al*.,[50] the absence of any observed wastewater treatment plants near to the sampling sites, the presence of untreated sewage discharge is the plausible source of coprostanol. We compared our results with other studies of sediments in Port regions (Table S8, SI section), and the concentrations of coprostanol were lower than those found in Montevideo Harbor, Uruguay,[51] but were very similar or higher than those found in Itajaí-Açú Estuarine, Brazil,[48] Santos Bay, Brazil,[52] Paranaguá Bay, Brazil,[53] and Patos Lagoon, Brazil.[54]

Sterol ratios

The diagnostic ratios for sterols were investigated and are also summarized in Table 2. These ratios were investigated considering that an individual analysis of coprostanol is not reliable for the determination of sewage contamination due to its probable production through *in situ* anaerobic hydrogenation of cholesterol.[55] The ratio of coprostanol/total sterols (R1) between 2-3% indicates moderately contaminated sediments, while when it is higher than 5-6% it indicates severe contamination. Most of our values are situated between 2-5% indicating contamination by sewage at a moderate level, with the region of sediment P2 being the most contaminated (19.05%).[49,56]

The R2 ratio (coprostanol/(coprostanol + cholestanol)) enabled an evaluation of the presence of sewage in the aquatic environment. Of the five sediments, only P2 presented a ratio between 0.5 and 1.0, which indicates that this sediment is heavily contaminated by sewage.[32] Regarding the remaining sediments, the values were found between 0.3 and 0.5, considered inconclusive.[47,57]

The R3 ratio (coprostanol + epicoprostanol/(coprostanol + epicoprostanol + cholestanol) was applied to compensate for a possible conversion of coprostanol into its epimer (epicoprostanol) by microbial activities, commonly detected in samples of digested sludge, suggesting that the presence of epicoprostanol ensures a total or partial degradation of sewage by microbial activity. The sediments presented a ratio between 0.39 and 0.66, which infer inconclusive results, as they are within the uncertainty limits from 0.3 to 0.7.[46,50,55,58]

The R4 (coprostanol/cholesterol) ratio is applied to differentiate the sources of contamination (anthropogenic or biogenic). Four sediments (P2, P3, P4 and P5) presented values greater than the threshold of 0.2, indicating a source of anthropogenic contamination.[50] The highest R4 value was found for the P2 sediment, which reinforced our conclusion the sediment was the most affected by sewage contamination.

The R5 (epicoprostanol/coprostanol) was calculated to determine if the sewage received any type of treatment before discharge, considering that epicoprostanol is derived from the aerobic decomposition of wastewater in treatment plants.[50] Only P2 presented a ratio below 0.2, indicating that the region had received untreated sewage discharge. The P1, P3, and P5 sediments presented ratios between 0.2 and 0.8, being inconclusive regarding treatment. The P4 sediment is noteworthy for being the only one to present a concentration of epicoprostanol higher than that of coprostanol (R5 > 0.8) suggesting that it received some partially treated sewage.[32,46,50,52]

In summary, the results obtained through the diagnostic ratios of sterols indicated that sediments P1, P3, P4, and P5 could be considered low to moderately contaminated, with a strong influence of biogenic OM. On the other hand,

the P2 sediment received input from untreated domestic sewage, dominated by human feces, resulting in a high level of environmental contamination. This contamination possibly originated from the shipyard facilities, such as bathrooms and kitchens, which had been in operation for about 6 years in this place.

Aliphatic hydrocarbons

Quantitative analyses of *n*-alkanes (*n*-C_{15} and *n*-C_{37}) and isoprenoids were performed using the GC-FID technique. Their individual concentrations are shown in Table S9 (SI section) and their total concentrations and diagnostic ratios are in Table 3. The sediments showed total concentrations of *n*-alkanes (Σ*n*-alkanes) ranging from 3.87 (P4) to 25.48 μg g^{-1} (P2). Notably, it was observed that samples P4 and P2 corresponded to the lowest and highest percentages of silt + clay, respectively. To examine the potential relationship between the accumulation of *n*-alkanes in the sediments and the fine particle size, a linear correlation analysis was conducted (Table S7, SI section).[11] The result of this correlation was not linear ($R^2 = 0.3246$) suggesting that particle size does not significantly influence the accumulation of *n*-alkanes.[8] The correlations of Σ*n*-alkanes with OM or TOC were also investigated and showed no linear relation (OM × Σ*n*-alkanes, $R^2 = 0.3552$; TOC × Σ*n*-alkanes, $R^2 = 0.5131$), which according to Gadelha *et al*.[10] indicate that they also do not influence the distribution of *n*-alkanes.

The wide variation in the Σ*n*-alkanes (Table 3) indicates a localized origin of hydrocarbons in the P2 sample.[11] In addition, long-chain *n*-alkanes with an odd number of carbon atoms were highly prevalent (*n*-C_{29}, *n*-C_{31}, *n*-C_{33}, and *n*-C_{35}, see Table S9), suggesting a significant contribution of biogenic hydrocarbons of continental origin (allochthone) derived from waxes of higher plants.[10,11,59] This corroborates the results from the TOC and sterol analyses, which also indicated a strong contribution of terrigenous material, whose source can be attributed to the mangrove present in the port region. Despite the moderately contaminated level of our samples, we observed higher values when comparing the Σ*n*-alkanes to those reported in other studies[8,53,60-65] conducted in estuarine regions with port activities and/or shipyards (Table S8, SI section).

The diagnostic ratios of *n*-alkanes are widely used to investigate the entry of hydrocarbon sources into aquatic environments.[9] The carbon preference index (CPI) is a parameter that relates the abundance of long-chain *n*-alkanes with the proportion of molecules possessing an even or odd number of carbon atoms.[4,9,10] All sediments presented CPI values close to 1, which means that the port region receives hydrocarbon inputs of petrogenic origin.[8,10] The TAR calculation is represented by the equation ($[C_{27} + C_{29} + C_{31}]/[C_{15} + C_{17} + C_{19}]$) and allows the identification of the predominance of hydrocarbons of aquatic origin (< 1) and terrigenous (> 1).[4,10,60,66] From the 5 sediments analyzed, only P1 and P5 presented a ratio less than 1, indicating a contribution of OM from aquatic sources (algae), for P2, P3, and P4 sediments, values greater than 1 were found, indicating a greater contribution of OM from terrigenous sources. This result reinforces the mix of contributions in the sedimentary OM that was also supported by the values of TOC/TN presented in Table 1.

Chlorophyll is the main source of two isoprenoid alkanes: pristane and phytane. They are widely found in crude oil and have greater resistance to degradation when compared to linear *n*-alkanes.[9,10] Pristane and phytane were detected in all samples, with the highest concentrations observed in sediment P1 (0.55 and 0.67 μg g^{-1}, respectively) and the lowest concentrations in sediment P4 (0.12 and 0.14 μg g^{-1}, respectively). Thus, the pristane/phytane ratio was investigated to determine the origin of these hydrocarbons. Values less than 1.5 for all samples were found, which indicates that the region suffers a strong influence from petrogenic sources.[10,60] The samples showed a pristane/phytane ratio similar to other results found in regions considered oil-contaminated, such as Ushuaia Bay, Argentina,[67] and Capibaribe Estuarine System, Brazil.[9]

Table 3. Total concentrations and diagnostic ratios of hydrocarbons of surface sediments from Port of Suape

Sample	Σ*n*-Alkane / (μg g^{-1})	CPI	TAR	Pr/Ph	Pr/*n*-C_{17}	Ph/*n*-C_{18}	ΣPAHs / (ng g^{-1})	Σ16PAHs / (ng g^{-1})	Flr/ (Flr + Pyr)	Ant/ (Ant+ Phen)	ΣLMM/ ΣHMM	B*a*A/ (B*a*A + Chry)	In*cd*P/ (In*cd*P + B*ghi*P)
P1	11.98	0.79	0.58	0.82	0.61	0.42	553.45	463.51	0.71	0.02	0.65	0.37	0.43
P2	25.48	1.28	3.32	0.86	0.59	0.61	644.87	511.94	0.73	0.03	0.34	0.41	0.44
P3	9.38	1.02	1.09	0.87	0.62	0.49	534.88	428.31	0.75	0.01	0.48	0.48	0.47
P4	3.77	0.57	1.01	0.84	0.74	0.53	236.27	210.59	0.8	NC	0.24	0.48	0.50
P5	3.87	0.61	0.93	0.84	0.73	0.48	313.72	281.68	0.76	NC	0.34	0.45	0.46

CPI: carbon preference index; TAR: terrestrial/aquatic ratio; Pr: pristane; Ph: phytane; Flr: fluoranthene; Pyr: Pyrene; Ant: anthracene; Phen: phenanthrene; PAHs: polycyclic aromatic hydrocarbons; LMM: low molecular mass; HMM: high molecular mass; B*a*A: benzo[*a*]anthracene; Chry: chrysene; In*cd*P: indene[1,2,3-*cd*]pyrene; B*ghi*P: benzo[*g*,*h*,*i*]perylene; NC: not calculated.

This further supports the idea that all sediments have been contaminated by oil or derivatives, potentially originating from port activities and navigation traffic (ships and boats).[8]

The Pr/*n*-C_{17} and Ph/*n*-C_{18} ratios were calculated as indicators of the biodegradation process in environments involving crude oil spills. Considering that *n*-C_{17} and *n*-C_{18} degrade faster than pristane, the increase in Pr/*n*-C_{17} ratio is noted in sediments that have undergone higher levels of biodegradation. For both ratios, all samples showed values less than 2, indicating that the oil was in the early stages of biodegradation, and thus had recently been introduced into the environment.[9,10,60]

Polycyclic aromatic hydrocarbon (PAHs)

A quantitative analysis of PAHs was conducted using GC-MS, and the concentrations of each specific compound are provided in Table S10 (SI section). A total of 19 PAHs were detected, with 16 of them considered priority contaminants by the United States Environmental Protection Agency (USEPA). These PAHs are well-known for their widespread occurrence and toxicity to the biota, and they are classified as likely to have carcinogenic properties.[68,69]

The ΣPAHs for 19 compounds (Table 3) ranged from 236.27 to 644.87 ng g^{-1}, with the highest concentration observed in P2 sediment, which was collected near the shipyards. Table S8 presents a comparison between the ΣPAHs found in the present study and other aquatic systems with port activities. It is observed that the maximum ΣPAHs value obtained in our study is lower than that reported in most other studies of marine systems with moderate to high contamination levels.[8,51,53,70,71]

The total concentration of the 16 PAHs (Σ16PAHs) (Table 3) ranged from 210.59 to 511.94 ng g^{-1}, with sample P2 exhibiting the highest value. This result suggests a moderate level of contamination in all sediments.[4] The Σ16PAHs found here is higher than in other regions with port activities and/or shipyards considered highly contaminated (Table S8, SI section).[8,51,61,72]

To determine the source of the PAHs we have calculated the diagnostic ratios (Table 3). These ratios involved comparing pairs of isomers, such as phenanthrene and anthracene (molecular mass (MM) = 178 g mol^{-1}), fluoranthene and pyrene (MM = 202 g mol^{-1}), indene[1,2,3-*cd*] pyrene, benzo[*g*,*h*,*i*]perylene (MM = 276 g mol^{-1}) and benzo[*a*]anthracene, and chrysene (MM = 228 g mol^{-1}).[73-76] All the ratios mentioned below are summarized in Frena *et al.*[8] and Yunker *et al.*[73] For fluoranthene/(fluoranthene + pyrene) all samples presented values above the threshold of 0.5, which suggests that the presence of PAHs in the port region originated from pyrogenic sources, such as the burning of grass, wood, or coal. For anthracene/(anthracene + phenanthrene) all samples had values lower than the threshold 0.1, indicating that sediments of the port region have received inputs of petrogenic origin. For benzo[*a*]anthracene/(benzo[*a*]anthracene + chrysene), all samples presented values above 0.35, indicating vehicular emission sources. For (indene[1,2,3-*cd*]pyrene/(indene[1,2,3-*cd*]pyrene + benzo[*g*,*h*,*i*]perylene)) all samples had values less than 0.5 suggesting oil combustion or vehicular emissions. The ΣLMM/ΣHMM of all sediments presented values lower than 1, which indicates sources of pyrogenic origin.

Considering that the results of the diagnostic ratios indicated the possibility of both pyrogenic and petrogenic origins on the sedimentary OM, it can be concluded that there is a contribution from mixed sources, with a greater predominance of petrogenic sources. The P2 sediment stood out due to its high concentration of PAHs and elevated specific diagnostic ratios, being considered the most affected by hydrocarbon contamination, which may be associated with the shipyard activities and navigation traffic.

Trace metals and As

In Table S11, the concentrations of Ag, Cd, and Sn were below the limit of quantification (LOQ) in all collected samples, and Co was only detected in the P1 sample, collected in the mouth of the Tatuoca River, which receives urban discharges from neighboring cities. The average concentration of trace metals followed the following decreasing order: Zn (44.2) > V (28.0) > Cr (22.0) > Cu and Pb (15.0) > As (1.0) > Co and Ni (6.0). The Zn was found to present the highest mean concentration (44 mg kg^{-1}), and also had the highest individual concentration in sediments P1 (94 mg kg^{-1}) and P2 (52 mg kg^{-1}), which may be associated with its use for the cathodic protection of structures related to shipyard activities that are subject to corrosion, such as hulls of ships and pipes.[77,78]

The assessment of environmental risks associated with trace metal contamination is commonly conducted by comparing sample concentrations with established sediment quality guidelines. The first one used in this study was resolution No. 454/2012, established by the National Environment Council of Brazil (CONAMA), which defines "the limit of low probability of adverse effects to biota (LPAE)".[79] Based on the limit, all samples showed concentration below the LPAE, indicating that they do not present a biological risk. The second guideline used was the Canadian Interim Sediment Quality Guidelines, which

categorizes sediments into threshold biological effect levels (TEL) and probable effect level (PEL), linked to negative biological impacts.[80] According to this guide, the majority of samples have concentrations below the TEL, which indicates a low probability of risks to the environment. However, two elements require attention. Cu levels in samples near the shipyards (P1 and P2) showed values between the TEL and PEL, indicating a moderate probability of risk to the biota. Moderate levels of As were also found in all samples in which it was quantified (P1, P4 and P5).

In addition to comparatives with sediment quality guides, several studies have utilized indices for determining anthropogenic contamination, such as: enrichment factor (EF), geoaccumulation index (Igeo), and contamination factor (CF).[14,36,81,82] The EF is commonly used to estimate trace metal pollution. For this parameter, normalization with Fe is often performed,[81-83] and calculations are performed by the equation 1:

$$EF = \frac{\left(\frac{C_n}{C_{Fe}}\right)_{sample}}{\left(\frac{C_n}{C_{Fe}}\right)_{background}} \quad (1)$$

where the numerator indicates the ratio between the concentration of the investigated element "n" and Fe in the sediment sample, while the denominator indicates the ratio between the background values of element "n" and Fe.[36,81,82] The background values used were based on the continental earth's crust.[84]

The EF values are summarized in Table S12 (SI section) and Figure 2a. These values show that most trace metals exhibit values between 0.02 and 2.0, indicating low enrichment, whose source can be associated with the regional composition of the rocks. Only As presented values between 1.83 and 2.50, indicating moderate enrichment, which may originate from anthropogenic contributions from the Port.[82,85]

The I_{geo} can estimate the degree of anthropogenic contamination by trace metals through the equation 2:

$$I_{geo} = \log_2\left(\frac{C_n}{1.5B_n}\right) \quad (2)$$

where C_n is the concentration of the element "n" in the sediment sample, B_n is the background value of the element "n" in the earth crust,[84] and 1.5 represents the matrix correction factor for background values resulting from lithological variations.[81,82,86,87]

Within the 7 contamination classes established for I_{geo}, ranging from class 0 (not contaminated, $I_{geo} < 0$) to class 6 (extremely contaminated, $I_{geo} > 5$), the most metals

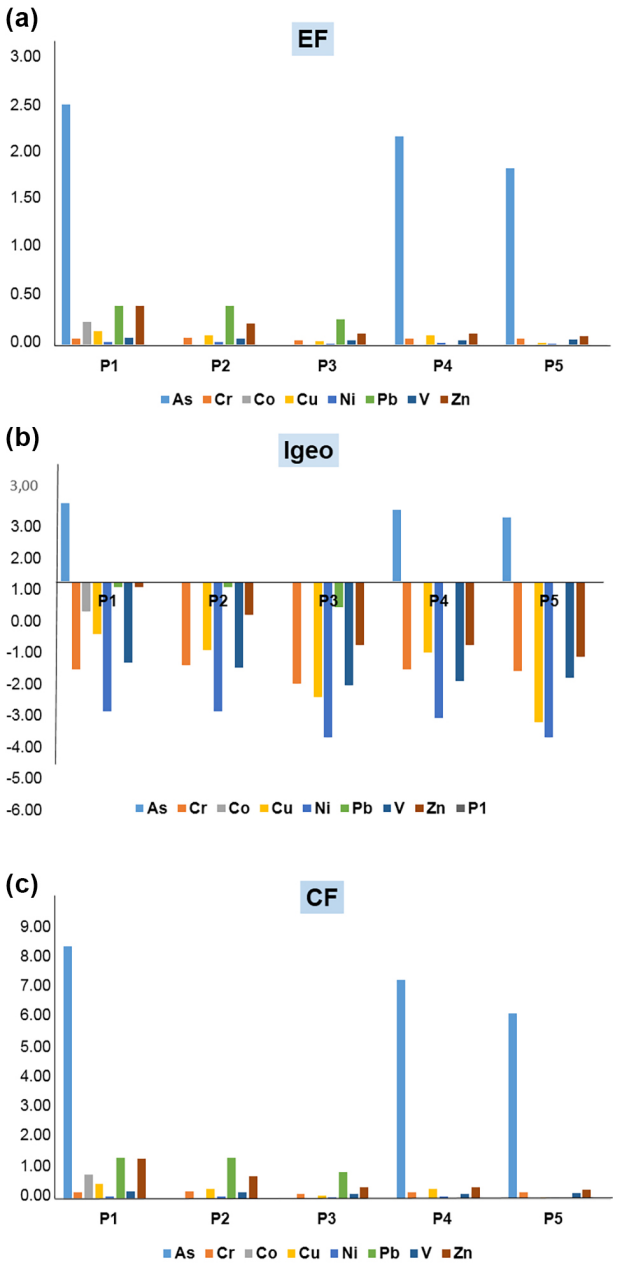

Figure 2. Results of contamination indexes by: (a) the enrichment factor (EF), (b) geoaccumulation index (I_{geo}), and (c) contamination factor (CF) of sediment samples from the Port of Suape.

studied presented values between –4.81 and –0.14, being classified as non-contaminated ($I_{geo} < 0$).[81,86,87] Once again, As presented higher values, being classified as moderately contaminated (class 3; $2 < I_{geo} < 3$) for samples P1, P4, and P5 (Figure 2b and Table S13).[81,85,87]

The CF was also calculated by comparing the concentration of the metal investigated in the sediment (C_n) and its background value (B_n).[84] As seen in Figure 2c and Table S14 (SI section), for Cr, Co, Cu, Ni, and V, low levels of contamination were identified for all samples ($CF \leq 1$). We also have found As presented the highest values of CF,

with sample P3 classified as considerably contaminated, and the other samples classified as highly contaminated. Notably, sample P1, located near one of the shipyards, in addition to presenting the highest values for As (CF = 8.33), also showed moderate contamination by Pb and Zn.[86,88]

In general, the study area showed low levels of contamination from most trace metals, with a decreasing trend of contamination following the order: As > Pb > Co > Zn > Cu > Cr > V > Ni. The identification of a moderate risk of contamination from As, particularly close to the shipyard, highlights the importance of continuous monitoring in the region and remedial actions, to guarantee environmental protection.

Statistical analysis

The PCA was carried out to investigate the correlation of OM, TOC, particle size, and contaminations by sterols, hydrocarbons, trace metals, and As, for the sediment sampling points. The trends and similarities between samples and variables can be analyzed through the proximity between the points in question: the closer, the greater the similarities.[8,45,89] The PCA results (Figure 3) reorganize the data into two components that explain 54.35% (PC1) and 20.64% (PC2) of the data variance, representing a total cumulative variance of 74.99%.

The P1 and P2 sediments exhibited positive scores along the PC1, while P3, P4, and P5 sediments showed negative scores. PC1 helps differentiate among the regions that are associated with activities from shipyards in the Port of Suape. In PC1, samples P1 and P2 are positively correlated to the percentages of silt + clay (C) having the highest values found. On the other hand, P3 and P4 have negative scores due to the lower values found for the silt + clay variables, and also due to their positive correlation to the sand contents (B), corroborating the effect of sediment dredging. Although the concentration of trace metals detected in this study was below the reference limits, there is a clear positive association between the higher metal content and P1 and P2 samples, which means that shipyard activities in the region contribute to the introduction of trace metals into the aquatic environment.

The P2 sediment showed the highest scores in PC1 and PC2, which was positively associated with OM, TOC, biomarkers/ratios of sewage contamination coprostanol/cholesterol), (coprostanol, coprostanol/(coprostanol + cholestanol), and hydrocarbons (Σ*n*-alkane, ΣPAH, Σ16PAH, CPI, TAR, anthracene/(anthracene + phenanthrene) and ΣLMM/ΣHMM), indicating that this was the region most affected by anthropogenic contamination, possibly resulting from shipyard activity and intense navigation traffic. In contrast, the P4 sediment has negative scores for the variables mentioned above, and for all trace metals (except arsenic), due to lower values obtained. P4 was also positively associated with the epicoprostanol/coprostanol ratio, indicating it as the sediment the least affected by contamination from sewage, hydrocarbons, and trace metals. The high values of the ratios of benzo[a]anthracene/(benzo[*a*]anthracene + chrysene) (Z) and fluoranthene/(fluoranthene + pyrene) observed in the P4 sediment suggest the prevalence of pyrolytic sources in this region.

In PC2, the P2 and P3 sediments are positively correlated to the Pr/Ph ratio as they present the highest values for this ratio. The P5 sediment is associated with

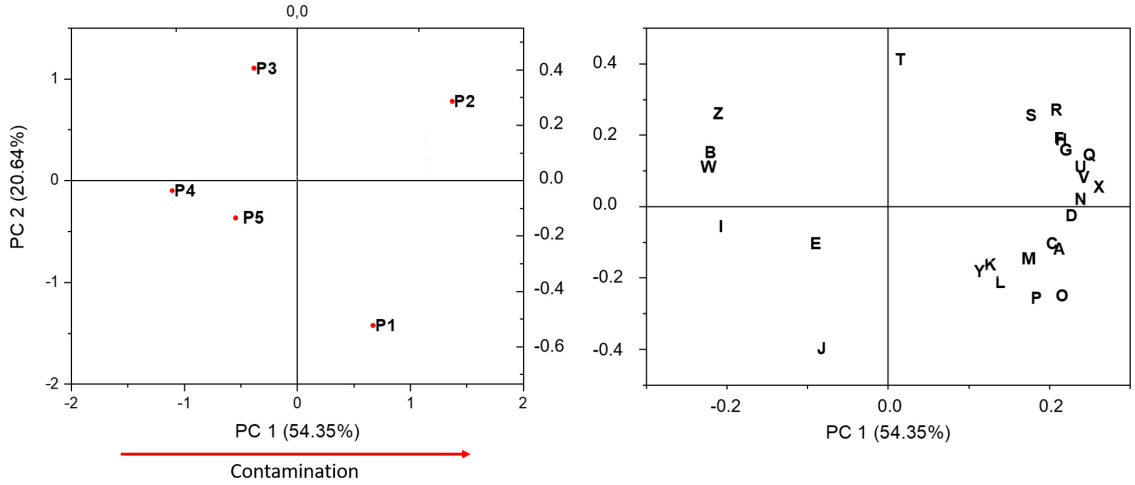

Figure 3. Principal component analysis (PCA) of the OM, TOC, particle size, sterols, hydrocarbons, trace metals, and As results for the surface sediments from Port of Suape. A: OM; B: sand; C: silt + clay; D: TOC; E: TOC/TN; F: coprostanol; G: (coprostanol/(coprostanol + colestanol)); H: coprostanol/cholesterol; I: epicoprostanol/coprostanol; J: arsenic; K: chromium; L: copper; M: nickel; N: lead; O: vanadium; P: zinc; Q: Σ*n*-alkane; R: carbon preference index (CPI); S: terrestrial/aquatic ratio (TAR); T: pristane/phytane; U: ΣPAHs; V: Σ16PAHs; W: (fluoranthene/(fluoranthene + pyrene)); X: (anthracene/(anthracene + phenanthrene)); Y: (Σlow molecular mass/Σhigh molecular mass); Z: (benzo[*a*]anthracene/(benzo[*a*]anthracene + chrysene)).

TOC/TN (E) contents as it presents the highest value for this variable, which is indicative of allochthonous OM (terrigenous). Figure 3 shows a tendency of increasing contamination from left to right in PC1 (red arrow) related to the results discussed above which means that the PCA was effective in differentiating the samples and confirming the indications of anthropogenic contamination in the sediments collected at the Port of Suape.

An HCA/heatmap was also generated (Figure 4) to investigate which variables exerted greater influence on the sediment samples through the differences in hues: reddish and bluish tones present greater and lesser weight, respectively.[6] The P2 sediment presented reddish tones for the biomarkers of sewage contamination (coprostanol/cholesterol), (coprostanol, coprostanol/(coprostanol + cholestanol) and by hydrocarbon results (Σ*n*-alkanes, ΣPAH, Σ16PAH, CPI, TAR, anthracene/(anthracene + phenanthrene) and ΣLMM/ΣHMM), as well as, for the OM and TOC. The heatmap reinforced the results discussed in this article that indicate the P2 sediment as the most affected by anthropogenic contamination. On the other hand, the P4 sediment is marked with a bluish hue for the same variables mentioned above, and warmer for the epicoprostanol/coprostanol ratio (I), corroborating the indication obtained in the PCA (Figure 3) that P4 was the least affected by anthropogenic contamination. Still, in P4, warm tones can be seen for the ratios benzo[*a*]anthracene/(benzo[*a*]anthracene + chrysene) (Z) and fluoranthene/(fluoranthene + pyrene) (W) highlighting the predominance of pyrolytic sources in this region, as also indicated by the PCA.

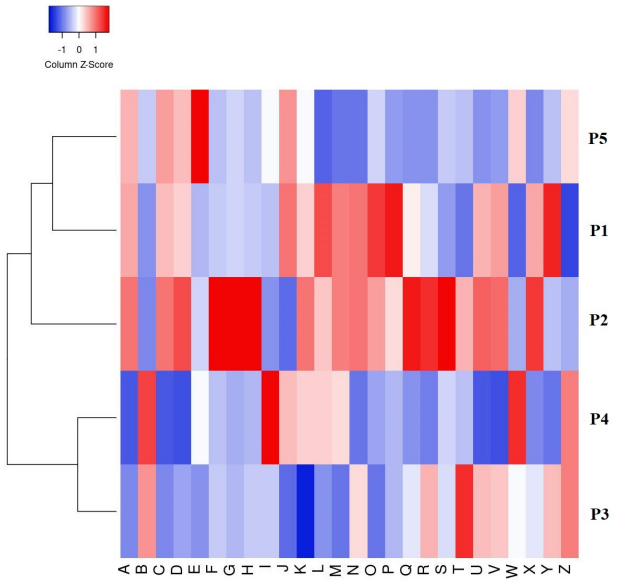

Figure 4. HCA/Heatmap of the data from bulk and advanced analyses of surface sediments from Port of Suape. Reddish and bluish tones present greater and lesser weight, respectively. A: OM; B: sand; C: silt + clay; D: TOC; E: TOC/TN; F: coprostanol; G: (coprostanol/(coprostanol + colestanol)); H: coprostanol/cholesterol; I: epicoprostanol/coprostanol; J: arsenic; K: chromium; L: copper; M: nickel; N: lead; O: vanadium; P: zinc; Q: Σ*n*-alkane; R: carbon preference index (CPI); S: terrestrial/aquatic ratio (TAR); T: pristane/phytane; U: ΣPAHs; V: Σ16PAHs; W: (fluoranthene/(fluoranthene + pyrene)); X: (anthracene/(anthracene + phenanthrene)); Y: (Σlow molecular mass/Σhigh molecular mass); Z: (benzo[*a*]anthracene/(benzo[*a*]anthracene + chrysene)).

All trace metals showed reddish tones for sediment samples taken from points P1 (mainly) and P2, indicating their high values presented by these variables, corroborating the indication that shipyards represent the gateway for these metals. These same sediments, as well as P5, presented reddish tones for silt + clay contents (C) and bluish tones for sand contents (B); the opposite can be seen in P3 and P4 sediments, showing the effect of sediment dredging. The P5 sediment presented the warmest shade for the variable TOC/TN (E), corroborating with the indications obtained throughout this study that terrigenous sources (mangrove forest) are predominantly responsible for OM. The results obtained from the HCA/Heatmap analysis are consistent with the findings derived from the PCA analysis shown in Figure 3, reinforcing the idea that the P2 sample was the most affected by anthropogenic contamination, while P4 was the least affected.

Conclusions

We performed a multi-geochemical characterization of sediments from the Port of Suape in northeastern Brazil to evaluate environmental chemical contamination in a multi-geochemical approach. Bulk analysis suggested that the region was subject to aquatic and terrigenous (predominant) OM. The analytical analyses indicated a low degree of contamination from sewage and petroleum, indicating an early stage of biodegradation. However, it is important to highlight that P1 and P2 sediments exhibited higher contamination levels, potentially attributed to the shipyard activities in the port region. Trace metals analysis also revealed low levels of contamination, except for As, which pointed to a moderate risk of contamination, mainly in P1 which is near the shipyard of the port, which demands greater attention. Thus, our findings presented here indicate a change in the quality of the sediments in the region and the need to implement effective remediation strategies to guarantee the environmental preservation of the area of one of the most important ports in Brazil.

Supplementary Information

Supplementary data (geographic location of sampling sites, analytical parameters for detection and quantification of sterols, AHs, PAHs and trace metals, infrared spectrum, linear correlations, comparison with other literature, and

absolute concentrations of AHs and PAHs of sediments samples collected in the Port of Suape, Northeast of Brazil) are available free of charge at http://jbcs.sbq.org.br as PDF file.

Author Contributions

Ana Flávia B. de Oliveira was responsible for methodology, analysis, statistical analysis, writing, and investigation; Bruna R. S. Gomes for methodology, analysis, writing, and investigation; Rebeca dos Santos França for methodology, analysis, and investigation; Thayane Cristina S. Moreira for writing; Alex S. Moraes for methodology, and investigation; Giovana A. Bataglion for methodology, analysis, investigation, writing-review and editing; Jandyson M. Santos for project coordinator, methodology, analysis, investigation, writing-review and editing.

Acknowledgments

This study was funded by Fundação de Amparo à Ciência e Tecnologia do Estado de Pernambuco (FACEPE). The authors would like to thank the multi-user analytical laboratories CLQM/UFS and LABMAQ/UFRPE. G. A. B. would like to thank Universidade Federal do Amazonas (UFAM), Conselho Nacional de Desenvolvimento Científico e Tecnológico (CNPq, Brazil), Coordenação de Aperfeiçoamento de Pessoal de Nível Superior (CAPES, Brazil, finance code 001) and Fundação de Amparo à Pesquisa do Estado do Amazonas (FAPEAM, Brazil) for financially support part of this study.

References

1. Gao, X.; Yang, Y.; Wang, C.; *Mar. Pollut. Bull.* **2012**, *64*, 1148. [Crossref]
2. de Abreu-Mota, M. A.; Barboza, C. A. M.; Bícego, M. C.; Martins, C. C.; *Chemosphere* **2014**, *103*, 156. [Crossref]
3. Sharma, E.; Das, S.; *Int. J. Environ. Waste Manage.* **2020**, *25*, 356. [Crossref]
4. Assunção, M. A.; Frena, M.; Santos, A. P. S.; dos Santos Madureira, L. A.; *Mar. Pollut. Bull.* **2017**, *119*, 439. [Crossref]
5. Frena, M.; Souza, M. R. R.; Damasceno, F. C.; Madureira, L. A. S.; Alexandre, M. R.; *Mar. Pollut. Bull.* **2016**, *109*, 619. [Crossref]
6. de Oliveira, A. F. B.; Gomes, B. R. S.; França, R. S. F.; Moraes, A. S.; Bataglion, G. A.; Santos, J. M.; *J. Braz. Chem. Soc.* **2022**, *33*, 163. [Crossref]
7. Souza, M. R. R.; Santos, E.; Suzarte, J. S.; do Carmo, L. O.; Soares, L. S.; Santos, L. G. G. V.; Júnior, A. R. V.; Krause, L. C.; Frena, M.; Damasceno, F. C.; Huang, Y.; da Rosa Alexandre, M.; *Mar. Pollut. Bull.* **2020**, *154*, 111067. [Crossref]
8. Frena, M.; Bataglion, G. A.; Sandini, S. S.; Kuroshima, K. N.; Eberlin, M. N.; Madureira, L. A. S.; *J. Braz. Chem. Soc.* **2017**, *28*, 603. [Crossref]
9. Maciel, D. C.; de Souza, J. R. B.; Taniguchi, S.; Bícego, M. C.; Schettini, C. A. F.; Zanardi-Lamardo, E.; *Mar. Pollut. Bull.* **2016**, *113*, 566. [Crossref]
10. Gadelha, L. G.; Frena, M.; Damasceno, F. C.; Santos, E.; Sant`Anna, M. V. S.; Vinhas, M. A.; Barreto, T. S. A.; Alexandre, M. R.; *Mar. Pollut. Bull.* **2019**, *149*, 110607. [Crossref]
11. de Melo, M. G.; de Castro, L. G.; Reis, L. A.; Costa, G. S.; da Silva, F. M. A.; Bolson, M. A.; Chaar, J. S.; Koolen, H. H. F.; Sargentini Jr., É.; Bataglion, G. A.; *Chemistry* **2020**, *2*, 274. [Crossref]
12. Rajeshkumar, S.; Liu, Y.; Zhang, X.; Ravikumar, B.; Bai, G.; Li, X.; *Chemosphere* **2018**, *191*, 626. [Crossref]
13. Campos, É. D. A.; da Silva, I. F.; Warden, C. F.; *Cienc. Saúde Coletiva* **2021**, *26*, 2253. [Crossref*]*
14. Algül, F.; Beyhan, M.; *Sci. Rep.* **2020**, *10*, 11782. [Crossref]
15. Alomary, A. A.; Belhadj, S.; *Environ. Monit. Assess.* **2007**, *135*, 265. [Crossref]
16. Dauvin, J. C.; Desroy, N.; Janson, A. L.; Vallet, C.; Duhamel, S.; *Mar. Pollut. Bull.* **2006**, *53*, 80. [Crossref]
17. Koening, M. L.; Leça, E. E.; Neumann-Leitão, S.; Macêdo, S. J.; *Braz. Achives Biol. Technol.* **2003**, *46*, 73. [Crossref]
18. Lemos, R. T. O.; de Carvalho, P. S. M.; Zanardi-Lamardo, E.; *Mar. Pollut. Bull.* **2014**, *82*, 183. [Crossref]
19. Oliveira, T. S.; Xavier, D. A.; Santos, L. D.; França, E. J.; Sanders, C. J.; Passos, T. U.; Barcellos, R. L.; *Mar. Pollut. Bull.* **2020**, *161*, 111794. [Crossref]
20. Rosa, A. H.; Rocha, J. C.; Furlan, M.; *Quim. Nova* **2000**, *23*, 472. [Crossref]
21. Suguio, K.; *Introdução à Sedimentologia*; Editora da Universidade de São Paulo: São Paulo, Brazil, 1973.
22. Rau, M.; Bataglion, G. A.; Madureira, L. A. D. S.; *Rev. Virtual Quim.* **2013**, *5*, 201. [Crossref]
23. de Melo, M. G.; da Silva, B. A.; Costa, G. S.; da Silva Neto, J. C. A.; Soares, P. K.; Val, A. L.; Chaar, J. S.; Koolen, H. H. F.; Bataglion, G. A.; *Environ. Pollut.* **2019**, *244*, 818. [Crossref]
24. Bataglion, G. A.; Meurer, E.; de Albergaria-Barbosa, A. C. R.; Bícego, M. C.; Weber, R. R.; Eberlin, M. N.; *Anal. Chem.* **2015**, *87*, 7771. [Crossref]
25. *Origin*, version 8.0; OriginLab Corporation, Origin Pro, Northampton, USA, 2019.
26. Heatmapper Expression; Wishart Research Group, University of Alberta, CA, 2012. [Link] accessed in August 2023
27. Dias, B. D. O.; Silva, C. A.; Mercês, E.; *Rev. Bras. Cienc. Solo* **2009**, *33*, 885. [Crossref]
28. Veerasingam, S.; Venkatachalapathy, R.; *Infrared Phys. Technol.* **2014**, *66*, 136. [Crossref]
29. Ng, W.; Malone, B. P.; Minasny, B.; *Geoderma* **2017**, *289*, 150. [Crossref]

30. Pavia, D. L.; Lampman, G. M.; Kriz, G. S.; Vyvyan, J. R.; *Introduction to Spectroscopy*, 2nd ed.; Cengage Learning: Orlando, 2015.
31. Alves, E. M.; Gallardo, A. L. C. F.; Kniess, C. T.; *Rev. Política Planejamento Regional* **2021**, *8*, 253. [Link] accessed in August 2023.
32. Hadlich, H. L.; Venturini, N.; Martins, C. C.; Hatje, V.; Tinelli, P.; Gomes, L. E. O.; Bernardino, A. F.; *Ecol. Indic.* **2018**, *95*, 21. [Crossref]
33. Gomes, A. O.; Azevedo, D. A.; *J. Braz. Chem. Soc.* **2003**, *14*, 358. [Crossref]
34. Mayer, L. M.; *Geochim. Cosmochim. Acta* **1994**, *58*, 1271. [Crossref]
35. Muniz, P.; Pires-Vanin, A. M. S.; Martins, C. C.; Montone, R. C.; Bícego, M. C.; *Mar. Pollut. Bull.* **2006**, *52*, 1098. [Crossref]
36. Souza, I. S.; Santos, F. R.; Martins, D. A.; Morais, P. C. V.; Gama, A. F.; Nascimento, R. F.; Cavalcante, R. M.; Abessa, D. M. S.; *Environ. Monit. Assess.* **2022**, *194*, 567. [Crossref]
37. Meyers, P.; *Org. Geochem.* **2003**, *34*, 261. [Crossref]
38. Santos, J. M.; dos Santos, L. O.; Costa, J. A. S.; Menezes, L. C. S.; Holanda, F. S. R.; Bellin, I. C.; *Rev. Virtual Quim.* **2015**, *7*, 2139. [Crossref]
39. Lima, E. A. M.: *Avaliação da Qualidade dos Sedimentos e Prognóstico Geoquímico Ambiental da Zona Estuarina do Rio Botafogo, Pernambuco;* PhD Thesis, Universidade Federal de Pernambuco, Pernambuco, Brazil, 2008. [Link] accessed in August 2023
40. Meyers, P. A.; *Org. Geochem.* **1997**, *27*, 213. [Crossref]
41. Hu, L.; Guo, Z.; Feng, J.; Yang, Z.; Fang, M.; *Mar. Chem.* **2009**, *113*, 197. [Crossref]
42. Grilo, C. F.; Neto, R. R.; Vicente, M. A.; de Castro, E. V. R.; Figueira, R. C. L.; Carreira, R. S.; *Appl. Geochemistry* **2013**, *38*, 82. [Crossref]
43. Bataglion, G. A.; Koolen, H. H. F.; Weber, R. R.; Eberlin, M. N.; *Int. J. Anal. Chem.* **2016**, ID 8361375. [Crossref]
44. Ranjan, R. K.; Routh, J.; Val Klump, J.; Ramanathan, A. L.; *Mar. Chem.* **2015**, *171*, 44. [Crossref]
45. Speranza, E. D.; Colombo, M.; Skorupka, C. N.; Colombo, J. C.; *Org. Geochem.* **2018**, *117*, 1. [Crossref]
46. Furtula, V.; Osachoff, H.; Derksen, G.; Juahir, H.; Colodey, A.; Chambers, P.; *Water Res.* **2012**, *46*, 1079. [Crossref]
47. Martins, C. C.; Cabral, A. C.; Barbosa-Cintra, S. C. T.; Dauner, A. L. L.; Souza, F. M.; *Environ. Pollut.* **2014**, *188*, 71. [Crossref]
48. Frena, M.; Bataglion, G. A.; Tonietto, A. E.; Eberlin, M. N.; Alexandre, M. R.; Madureira, L. A. S.; *Sci. Total Environ.* **2016**, *544*, 432. [Crossref]
49. Tolosa, I.; Mesa, M.; Alonso-Hernandez, C. M.; *Mar. Pollut. Bull.* **2014**, *86*, 84. [Crossref]
50. Bujagić, I. M.; Grujić, S.; Jauković, Z.; Laušević, M.; *Environ. Pollut.* **2016**, *213*, 76. [Crossref]
51. Muniz, P.; Venturini, N.; Martins, C. C.; Munshi, A. B.; García-Rodríguez, F.; Brugnoli, E.; Dauner, A. L. L.; Bícego, M. C.; García-Alonso, J.; *Braz. J. Oceanogr.* **2015**, *2015*, 311. [Crossref]
52. Martins, C. C.; Gomes, F. B. A.; Ferreira, J. A.; Montone, R. C.; *Quim. Nova* **2008**, *31*, 1008. [Crossref]
53. Bet, R.; Bícego, M. C.; Martins, C. C.; *Mar. Pollut. Bull.* **2015**, *95*, 183. [Crossref]
54. Martins, C. D. C.; Fillmann, G.; Montone, R. C.; *J. Braz. Chem. Soc.* **2007**, *18*, 106. [Crossref]
55. Tse, T. J.; Codling, G.; Jones, P. D.; Thoms, K.; Liber, K.; Giesy, J. P.; Wheater, H.; Doig, L. E.; *Chemosphere* **2014**, *103*, 299. [Crossref]
56. Hatcher, P. G.; McGillivary, P. A.; *Environ. Sci. Technol.* **1979**, *13*, 1225. [Crossref]
57. Carreira, R. S.; Araújo, M. P.; Costa, T. L. F.; Spörl, G.; Knoppers, B. A.; *Mar. Chem.* **2011**, *127*, 1. [Crossref]
58. He, D.; Zhang, K.; Tang, J.; Cui, X.; Sun, Y.; *Sci. Total Environ.* **2018**, *636*, 787. [Crossref]
59. do Nascimento, M. G.: *Marcadores Orgânicos Geoquímicos em Sedimentos Superficiais da Plataforma Rasa Paranaense;* MSc Dissertation, Universidade Federal do Paraná, Paraná, Brazil, 2011. [Link] accessed in August 2023
60. Wang, X. C.; Sun, S.; Ma, H. Q.; Liu, Y.; *Mar. Pollut. Bull.* **2006**, *52*, 129. [Crossref]
61. Punyu, V. R.; Harji, R. R.; Bhosle, N. B.; Sawant, S. S.; Venkat, K.; *J. Earth Syst. Sci.* **2013**, *122*, 467. [Crossref]
62. Nishigima, F. N.; Weber, R. R.; Bicego, M. C.; *Mar. Pollut. Bull.* **2001**, *42*, 1064. [Crossref]
63. Carvalho, A. C. B.; Moreira, V. A.; Vicente, M. C.; Bernardes, M. C.; Bidone, E. D.; Sabadini-Santos, E.; *Estuarine, Coastal Shelf Sci.* **2021**, *261*, 107548. [Crossref]
64. A. Mohamed, L.; El Zokm, G. M.; El Deeb, K. Z.; A. Okbah, M.; *Egypt. J. Aquat. Res.* **2016**, *42*, 375. [Crossref]
65. Buruaem, L. M.; Taniguchi, S.; Sasaki, S. T.; Bícego, M. C.; Costa-Lotufo, L. V.; Abessa, D. M. S.; *Environ. Earth Sci.* **2016**, *75*. [Crossref]
66. Celino, J. J.; Veiga, I. G.; Trigüis, J. A.; Queiroz, A. F. S.; *Braz. J. Aquat. Sci. Technol.* **2008**, *12*, 31. [Crossref]
67. Commendatore, M. G.; Nievas, M. L.; Amin, O.; Esteves, J. L.; *Mar. Environ. Res.* **2012**, *74*, 20. [Crossref]
68. Maioli, O. L. G.; Rodrigues, K. C.; Knoppers, B. A.; Azevedo, D. A.; *J. Braz. Chem. Soc.* **2010**, *21*, 1543. [Crossref]
69. United States EPA; *J. Toxicol. Cutan. Ocul. Toxicol.* **1999**, *18*, 141. [Crossref]
70. Notar, M.; Leskovšek, H.; Faganeli, J.; *Mar. Pollut. Bull.* **2001**, *42*, 36. [Crossref]
71. Medeiros, P. M.; Bícego, M. C.; *Mar. Pollut. Bull.* **2004**, *49*, 761. [Crossref]
72. Vitali, F.; Mandalakis, M.; Chatzinikolaou, E.; Dailianis, T.; Senatore, G.; Casalone, E.; Mastromei, G.; Sergi, S.; Lussu, R.; Arvanitidis, C.; Tamburini, E.; *Front. Mar. Sci.* **2019**, *6*, 590. [Crossref]

73. Yunker, M. B.; Macdonald, R. W.; Vingarzan, R.; Mitchell, H.; Goyette, D.; Sylvestre, S.; *Org. Geochem.* **2002**, *33*, 489. [Crossref]
74. Tay, C. K.; Biney, C. A.; *Environ. Earth Sci.* **2013**, *68*, 1773. [Crossref]
75. Jeanneau, L.; Faure, P.; Jardé, E.; *J. Chromatogr. A* **2007**, *1173*, 1. [Crossref]
76. Meire, R. O.; Azeredo, A.; Torres, J. P. M.; *Oecologia Bras.* **2007**, *11*, 188. [Crossref]
77. Moreira, L. B.; Castro, Í. B.; Hortellani, M. A.; Sasaki, S. T.; Taniguchi, S.; Petti, M. A. V.; Fillmann, G.; Sarkis, J. E. S.; Bícego, M. C.; Costa-Lotufo, L. V.; Abessa, D. M. S.; *Ecotoxicol. Environ. Saf.* **2017**, *135*, 137. [Crossref]
78. Barbarin, M.; Turquois, C.; Dubillot, E.; Huet, V.; Churlaud, C.; Muttin, F.; Thomas, H.; *Sci. Total Environ.* **2022**, *857*, 159244. [Crossref]
79. Conselho Nacional do Meio Ambiente (CONAMA); Resolução No. 454, de 01 de Novembro de 2012, *Estabelece as Diretrizes Gerais e os Procedimentos Referenciais para o Gerenciamento do Material a ser Dragado em Águas sob Jurisdição Nacional*; Diário Oficial da União (DOU), Brasília, Brazil, 2012. [Link] accessed in August 2023
80. Canadian Sediment Quality Guidelines for the Protection of AquaticLife, https://www.pla.co.uk/Environment/Canadian-Sediment-Quality-Guidelines-for-the-Protection-of-Aquatic-Life, accessed in August 2023.
81. Salam, M. A.; Paul, S. C.; Shaari, F. I.; Rak, A. E.; Ahmad, R. B.; Kadir, W. R.; *Hydrology* **2019**, *6*, 30. [Crossref]
82. Mirza, R.; Moeinaddini, M.; Pourebrahim, S.; Zahed, M. A.; *Mar. Pollut. Bull.* **2019**, *145*, 526. [Crossref]
83. Ali, U.; Malik, R. N.; Syed, J. H.; Mehmood, C. T.; Sánchez-García, L.; Khalid, A.; Chaudhry, M. J. I.; *Environ. Sci. Pollut. Res.* **2015**, *22*, 4316. [Crossref]
84. Taylor, S. R.; *Geochim. Cosmochim. Acta* **1964**, *28*, 1273. [Crossref]
85. Xu, F.; Liu, Z.; Cao, Y.; Qiu, L.; Feng, J.; Xu, F.; Tian, X.; *Catena* **2017**, *150*, 9. [Crossref]
86. Negahban, S.; Mokarram, M.; *Earth Space Sci.* **2021**, *8*, e2020EA001120. [Crossref]
87. Muller, G.; *GeoJournal.* **1969**, 108. [Link] accessed in August 2023
88. Hakanson, L.; *Water Res.* **1980**, *14*, 975. [Crossref]
89. Gomes, B. R. S.; França, R. S.; Moraes, A. S.; Bataglion, G. A.; Santos, J. M.; *Quim. Nova* **2022**, *45*, 1205. [Crossref]

Submitted: May 31, 2023
Published online: September 11, 2023